

a dynamic process. The fact that the signals at 6.12 and 5.93 ppm (*m*-H of PMes) remained separate at $T < 0^\circ\text{C}$ further confirms that **2** exists in solution in conformation ii of Figure 4. It follows that the collapse of the spectrum to singlets that indicate just one type of boron mesityl and one type of phosphorus mesityl, at ca. 120°C , implies that the rapid rotation around both types of B-P bond is occurring at this temperature. In effect, the variable-temperature studies do not distinguish between the rotations around the two types of B-P bonds, since this would involve the detection of rotamers i and iii of Figure 4 in the variable-temperature experiments. The observation of only three *o*-Me group resonances, one for the phosphorus mesityls and two attributable to the mesityl on boron, does not occur. Quite possibly, the two barriers are very close in energy, and this is consistent with the similar average B-P bond lengths for the inner and outer B-P bonds. The average energy value for the barriers (near 18 kcal mol^{-1}) is entirely consistent with the numbers measured recently

in other B-P molecules.¹³ The magnitude of this barrier demonstrates that noncyclic extended B-P arrays may exhibit extensive and moderately strong π -electron delocalization.

Acknowledgment. We thank the National Science Foundation for financial support.

Registry No. 1, 112059-41-3; 2, 136805-17-9; 2^{9/2}pentane, 136805-18-0; MesPH₂, 1732-66-7; Mes₂BF, 436-59-9; PhBCl₂, 873-51-8; Mes₂BPHMes·Li, 130417-23-1.

Supplementary Material Available: Description of the variable-temperature ¹H NMR spectra of **2**, full tables of data collection parameters, atomic coordinates and isotropic displacement coordinates for non-hydrogen atoms, bond distances and angles, hydrogen coordinates, anisotropic thermal parameters, hydrogen atom coordinates and isotropic displacement coordinates, and ¹H NMR data assignments, and a figure of the variable-temperature ¹H NMR spectrum of **2** in C₇D₈ (21 pages). Ordering information is given on any current masthead page.

Carbon-Sulfur Bond Cleavage with a Loss of Stereochemistry in the Ring Opening of *trans*-2,4-Diphenylthietane by Os₃(CO)₁₀(NCMe)₂

Richard D. Adams* and Michael P. Pompeo

Department of Chemistry, University of South Carolina, Columbia, South Carolina 29208

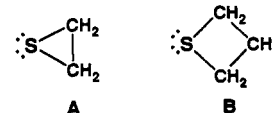
Received June 25, 1991

The reaction of Os₃(CO)₁₀(NCMe)₂ with *trans*-2,4-diphenylthietane (2,4-DPT) at 25°C resulted in the formation of two isomers, *cis*- and *trans*-Os₃(CO)₁₀[μ -SC(H)PhCH₂C(H)Ph] (**1**), in a combined yield of 76%. The *cis* product was characterized by single-crystal X-ray diffraction analysis and was found to contain a thiametalladiphenylcyclopentane ring formed by the opening of the thietane ring. The *cis* and *trans* isomers differ in the orientation of their phenyl substituents. The isomers are formed in approximately equal amounts in the early stages of the reaction, but the *trans* isomer subsequently slowly isomerizes to the *cis* isomer. The observed loss in stereochemistry at the carbon center is attributed to a stepwise ring-opening mechanism. When compound **1** was heated to 97°C under a CO atmosphere, five compounds were formed: Os₃(CO)₁₀[μ -SC(H)PhC(H)=C(H)Ph](μ -H) (**2**) (22%), Os₂(CO)₇[μ -SC(H)(C₆H₄)CH₂CH₂Ph] (**3**) (11%), Os₃(CO)₁₁[μ -SC(H)PhCH₂C(H)Ph] (**4**) (39%), H₂Os₃(CO)₁₇(μ_3 -S)(μ_4 -S) (**5**) (a trace amount), and Os₃(CO)₁₂. Compounds **3** and **5** and the known compound Os₃(CO)₉(μ_3 -CO)(μ_3 -S) (**6**) were obtained in better yields by heating **2** to 125°C in octane solvent. Compounds **2-4** were characterized by IR, ¹H NMR, and single-crystal X-ray diffraction analyses. Compound **2** is an isomer of **1** and contains a diphenylpropanethiolate and hydride ligand formed by a " β -elimination" transformation of the ring system in **1**. The mechanism of this transformation was not established. Compound **3** contains only two metal atoms and an ortho-metalated phenyl ring. Compound **4** is a CO adduct of **1** formed by the cleavage of the sulfur-bridged metal-metal bond. Crystallographic data are as follows. *cis*-**1**: space group *P*₂₁/*c*, *a* = 8.674 (2) Å, *b* = 35.09 (1) Å, *c* = 9.449 (2) Å, β = 106.41 (1)°, *Z* = 4, 2053 reflections, *R* = 0.033. **2**: space group *C*2/*c*, *a* = 13.845 (2) Å, *b* = 14.545 (4) Å, *c* = 28.907 (6) Å, β = 98.88 (1)°, *Z* = 8, 2519 reflections, *R* = 0.027. **3**: space group *P*₂₁/*c*, *a* = 8.337 (1) Å, *b* = 17.311 (4) Å, *c* = 16.409 (3) Å, β = 100.82 (1)°, *Z* = 4, 2299 reflections, *R* = 0.036. **4**: space group *P*₁, *a* = 14.319 (2) Å, *b* = 17.794 (5) Å, *c* = 12.257 (4) Å, α = 106.69 (2)°, β = 90.74 (2)°, γ = 82.56 (2)°, *Z* = 4, 4020 reflections, *R* = 0.041.

Introduction

The ring-opening cleavage of carbon-sulfur bonds in sulfur-containing heterocycles is of great interest because it is believed to be a key step in the purification of fossil fuels by the process of hydrodesulfurization.¹ Strained-

ring thioethers, such as thiirane **A** and thietane **B**, have



attracted attention since the release of ring strain in these molecules makes their carbon-sulfur bond cleavage processes more facile. Thiiranes and thietanes are known to undergo facile desulfurization on some metal surfaces.^{1b,2}

(1) (a) Angelici, R. J. *Acc. Chem. Res.* 1988, 21, 387. (b) Friend, C. M.; Roberts, J. T. *Acc. Chem. Res.* 1988, 21, 394. (c) Markel, E. J.; Schrader, G. L.; Sauer, N. N.; Angelici, R. J. *J. Catal.* 1989, 116, 11. (d) Prins, R.; De Beer, V. H. H.; Somorjai, G. A. *Catal. Rev. Sci. Eng.* 1989, 31, 1.

Theoretical studies have indicated that the ring opening of thietanes on molybdenum surfaces is preferred by interactions involving more than one metal atom.³

In recent studies we have shown that coordinated thietanes undergo facile ring opening in metal carbonyl cluster complexes.⁴⁻⁷ Evidence for both photochemical^{4,5} and nucleophile-assisted^{6,7} processes has been obtained.

We have now discovered that *trans*-2,4-diphenylthietane undergoes a facile thermal ring opening that is accompanied by a loss in stereochemistry in its reaction with $\text{Os}_3(\text{CO})_{10}(\text{NCMe})_2$ at 25 °C. These results are described in this report.

Experimental Section

General Data. Reagent grade solvents were stored over 4-Å molecular sieves. The compounds $\text{Os}_3(\text{CO})_{11}\text{NCMe}$,⁸ $\text{Os}_3(\text{CO})_{10}(\text{NCMe})_2$,⁹ and 2,4-diphenylthietane¹⁰ (2,4-DPT) were prepared by the published procedures. *trans*-2,4-DPT (mp 101 °C; lit.¹⁰ mp 102 °C, a racemic mixture) was separated from the *cis*-2,4-DPT isomer by repeated fractional crystallizations from petroleum ether. The *cis*-2,4-DPT isomer could not be completely purified and was used containing up to 30% *trans*-2,4-DPT. All reactions were performed under a nitrogen atmosphere unless specified otherwise. Infrared spectra were recorded on a Nicolet 5DXB FTIR spectrophotometer. ¹H NMR spectra were run on either a Bruker AM-300 or AM-500 spectrometer operating at 300 and 500 MHz, respectively. Mass spectra were obtained on a VG Model 70SQ spectrometer by using electron impact ionization. Chromatographic separations were performed in air on Whatman 60-Å silica gel (0.25 mm) F₂₅₄ plates. Silica gel (70–230 mesh, 60 Å) was purchased from Aldrich. Elemental analyses were performed by Oneida Research Services, Whitesboro, NY.

Reaction of $\text{Os}_3(\text{CO})_{10}(\text{NCMe})_2$ with 2,4-DPT. A. One equivalent (24.2 mg, 0.107 mmol) of *trans*-2,4-DPT dissolved in 5 mL of CH_2Cl_2 was added dropwise to a solution of $\text{Os}_3(\text{CO})_{10}(\text{NCMe})_2$ (100 mg, 0.107 mmol) in 20 mL of CH_2Cl_2 at 25 °C. The color of the solution changed from bright yellow to dark red. After being stirred for 1 h, the solution was reduced in volume and chromatographed on a silica gel column (25 × 2.5 cm). Elution with an 8/1 hexane/ CH_2Cl_2 solvent mixture yielded 88 mg (76%) of dark red $\text{Os}_3(\text{CO})_{10}[\mu\text{-SC}(\text{H})\text{PhCH}_2\text{C}(\text{H})\text{Ph}]$ (1). A ¹H NMR spectrum of 1 taken immediately after chromatography (2 h after starting the reaction) displayed resonances for both *cis*- and *trans*-1 isomers in a 1.6/1 ratio (by integration). Due to its spontaneous isomerization to the *cis* isomer (see below), *trans*-1 could not be isolated in a pure form either by TLC or by fractional crystallization. IR, $\nu(\text{CO})$ (cm^{-1}) in hexane for a mixture of *cis*- and *trans*-1: 2106 (m), 2059 (s), 2048 (m), 2022 (vs), 2000 (m), 1989 (m), 1940 (w). ¹H NMR (δ in CDCl_3) for *cis*-1: 7.41–6.99 (m, 10 H), 4.33 (dd, 1 H, ³*J*_{H-H} = 5.2 Hz, ³*J*_{H-H} = 13 Hz), 3.74 (ddd, 1 H, ³*J*_{H-H} = 2.4 Hz, ³*J*_{H-H} = 5.2 Hz, ²*J* = 13.7 Hz), 3.29 (dd, 1 H, ³*J*_{H-H} = 2.4 Hz, ³*J*_{H-H} = 13 Hz), 3.01 (dt, 1 H, ³*J*_{H-H} = 13.1 Hz, ²*J*_{H-H} = 13.5 Hz). ¹H NMR (δ in CDCl_3) for *trans*-1: 7.44–6.98 (m, 10 H), 5.04 (dd, 1 H, ³*J*_{H-H} = 4.6 Hz, ³*J*_{H-H} = 6.7 Hz), 3.68 (dd, 1 H, ³*J*_{H-H} = 4.6 Hz, ³*J*_{H-H} = 9.9 Hz), 3.58 (dt, 1 H, ³*J*_{H-H} = 4.7 Hz, ³*J*_{H-H} = 4.7 Hz, ²*J*_{H-H} = 14.6 Hz), 2.75 (ddd, 1 H, ³*J*_{H-H} = 6.7 Hz, ³*J*_{H-H} = 9.7 Hz, ²*J*_{H-H} = 14.6 Hz). Anal. Calcd for *cis*-1: C, 27.88; H, 1.31. Found: C, 27.88; H, 1.24.

B. One equivalent (21.7 mg, 0.096 mmol) of a mixture of *cis*- and *trans*-2,4-DPT (>70% *cis*) dissolved in 5 mL of CH_2Cl_2 was added dropwise to a solution of $\text{Os}_3(\text{CO})_{10}(\text{NCMe})_2$ (90 mg, 0.096

mmol) in 40 mL of CH_2Cl_2 at 25 °C. After being stirred for 1 h, the solution was reduced in volume and chromatographed on a silica gel column (25 × 2.5 cm). Elution with an 8/1 (v/v) hexane/ CH_2Cl_2 solvent mixture yielded an isomeric mixture of 1 (93 mg, 89%). Crystals of the isomer *cis*-1 were grown for X-ray diffraction and elemental analysis from this sample.

Reaction of $\text{Os}_3(\text{CO})_{10}(\text{NCMe})_2$ with *trans*-2,4-DPT in the Absence of Light. A solution of $\text{Os}_3(\text{CO})_{10}(\text{NCMe})_2$ (10 mg, 0.011 mmol) in 10 mL of CH_2Cl_2 was placed in a 25-mL one-neck flask equipped with a rubber septum. The flask was purged with N_2 , and the outside was wrapped completely with aluminum foil. A solution of *trans*-2,4-DPT (2.5 mg, 0.011 mmol) in 0.5 mL of CH_2Cl_2 was added to the flask via syringe. The mixture was stirred by hand for 15 s, and an aliquot of the solution was removed via syringe for IR analysis. An IR spectrum of the solution (taken in a dark room) clearly indicated the formation of large amounts of 1. IR, $\nu(\text{CO})$ (cm^{-1}) in CH_2Cl_2 : 2107 (m), 2060 (s), 2041 (m), 2021 (s), 1983 (m), 1942 (w). After 1 h, the solvent was removed in vacuo and the residue analyzed by ¹H NMR in CDCl_3 . The spectrum displayed resonances for both *cis*- and *trans*-1. TLC of the residue yielded 6.1 mg of 1 (52%).

Thermolysis of 1 in the Presence of CO. A heptane solution of *cis*-1 (60 mg, 0.056 mmol) was heated to 97 °C under an atmosphere of carbon monoxide for 1 h. The color of the solution changed from red to yellow. The solvent was removed in vacuo and the residue chromatographed by TLC. A 4/1 (v/v) hexane/ CH_2Cl_2 solvent mixture was used to separate the following compounds in order of elution: yellow $\text{Os}_3(\text{CO})_{10}[\mu\text{-SC}(\text{H})\text{PhC}(\text{H})=\text{C}(\text{H})\text{Ph}](\mu\text{-H})$ (2) (13 mg, 22%), pale yellow $\text{Os}_2(\text{CO})_7[\mu\text{-SC}(\text{H})(\text{C}_6\text{H}_4)\text{CH}_2\text{CH}_2\text{Ph}]$ (3) (5.0 mg, 11%), orange $\text{Os}_3(\text{CO})_{11}[\mu\text{-SC}(\text{H})\text{PhCH}_2\text{C}(\text{H})\text{Ph}]$ (4) (24 mg, 39%), and a trace of red $\text{H}_2\text{Os}_6(\text{CO})_{17}(\mu_3\text{-S})(\mu_4\text{-S})$ (5). $\text{Os}_3(\text{CO})_{12}$ (3 mg), identified by IR, was recovered from the reaction mixture. Data for 2 follow. IR, $\nu(\text{CO})$ (cm^{-1}) in hexane: 2109 (m), 2069 (vs), 2060 (s), 2025 (vs), 2018 (s), 2001 (s), 1990 (m), 1984 (w). ¹H NMR (δ in CDCl_3): 7.46–7.22 (m, 10 H), 6.46 (d, 1 H, ³*J*_{H-H} = 15.7 Hz), 6.28 (dd, 1 H, ³*J*_{H-H} = 8.3, 15.7 Hz), 3.64 (d, 1 H, ³*J*_{H-H} = 8.3 Hz). Anal. Calcd for 2: C, 27.88; H, 1.31. Found: C, 27.71; H, 1.23. Data for 3 follow. IR, $\nu(\text{CO})$ (cm^{-1}) in hexane: 2119 (m), 2065 (vs), 2044 (vs), 2034 (s), 2009 (s), 1988 (m), 1984 (m). ¹H NMR (δ in CDCl_3): 7.74 (m, 1 H), 7.30 (m, 5 H), 7.04 (m, 1 H), 6.87 (m, 2 H), 3.97 (dd, 1 H, ³*J*_{H-H} = 4.6 Hz, 9.4 Hz), 2.99 (t, 2 H, ³*J*_{H-H} = 8.2 Hz), 2.27 (m, 1 H), 2.07 (m, 1 H). Mass spectral analysis (70 eV, 100 °C): *m/e* for ¹⁹²Os = 802 – 28*x*, *x* = 0–7 ($[\text{M}]^+ - x(\text{CO})$). Data for 4 follow. IR, $\nu(\text{CO})$ (cm^{-1}) in hexane: 2126 (m), 2082 (s), 2049 (vs), 2042 (s), 2027 (m), 2009 (m), 1996 (s), 1988 (m), 1975 (w), 1967 (w). ¹H NMR (δ in CDCl_3): 7.34–7.19 (m, 10 H), 4.48 (dd, 1 H, ³*J*_{H-H} = 5.4, 12.5 Hz), 3.29 (dd, 1 H, ³*J*_{H-H} = 3.2, 12.5 Hz), 2.24 (ddd, 1 H, ³*J*_{H-H} = 3.2, 5.4 Hz, ²*J*_{H-H} = 12.5 Hz), 2.14 (dt, 1 H, ²*J*_{H-H} = ³*J*_{H-H} = 12.5 Hz). Anal. Calcd for 4: C, 28.26; H, 1.28. Found: C, 28.73; H, 1.30.

Thermolysis of 2 in the Presence of CO. A solution of 2 (26 mg, 0.024 mmol) in 25 mL of octane was heated to 125 °C for 2 h under an atmosphere of carbon monoxide. The color of the solution changed from yellow to red. Workup as above yielded unreacted 2 (7.3 mg), 3 (4.8 mg, 35%), $\text{Os}_3(\text{CO})_9(\mu_3\text{-CO})(\mu_3\text{-S})$ (6)¹² (5.5 mg, 36%), and 5 (5.4 mg, 19%). Yields are based on amount of 2 consumed. No $\text{Os}_3(\text{CO})_{12}$ was observed to form from this reaction.

Thermolysis of 4 in the Presence of CO. A solution of 4 (30 mg, 0.027 mmol) in 25 mL of heptane was heated to 97 °C for 1.5 h under an atmosphere of carbon monoxide. During the course of the reaction, the solution color changed from orange to red and then back to orange due to the in situ formation of 1, which was detected by an IR analysis of the solution taken after 0.5 h. Workup as above yielded 2 (7.5 mg, 33%), 3 (5.0 mg, 30%), and unreacted 4 (7.0 mg). Yields are based on amount of 4 consumed. $\text{Os}_3(\text{CO})_{12}$ (0.5 mg) was recovered from the reaction mixture.

Observation of the Reaction of $\text{Os}_3(\text{CO})_{10}(\text{NCMe})_2$ with *trans*-2,4-DPT by ¹H NMR. A solution of $\text{Os}_3(\text{CO})_{10}(\text{NCMe})_2$

(2) (a) Roberts, J. T.; Friend, C. M. *J. Am. Chem. Soc.* 1987, 109, 7899.

(b) Roberts, J. T.; Friend, C. M. *J. Am. Chem. Soc.* 1987, 109, 3872.

(3) Calhorda, M. J.; Hoffmann, R.; Friend, C. M. *J. Am. Chem. Soc.* 1988, 110, 749.

(4) Adams, R. D.; Pompeo, M. P. *Organometallics* 1990, 9, 1718.

(5) Adams, R. D.; Pompeo, M. P. *Organometallics* 1990, 9, 2651.

(6) Adams, R. D.; Pompeo, M. P. *J. Am. Chem. Soc.* 1991, 113, 1619.

(7) Adams, R. D.; Belinski, J. A.; Pompeo, M. P. *Organometallics* 1991, 10, 2539.

(8) Johnson, B. F. G.; Lewis, J.; Pippard, D. J. *Organomet. Chem.* 1978, 160, 263; 1981, 213, 249.

(9) Aime, S.; Deeming, A. J. *J. Chem. Soc., Dalton Trans.* 1983, 1809.

(10) Dodson, R. M.; Jancis, E. H.; Klose, G. J. *Org. Chem.* 1970, 8, 2520.

(11) Adams, R. D.; Horvath, I. T.; Mathur, P.; Segmüller, B. E. *Organometallics* 1983, 2, 996.

(12) Adams, R. D.; Horvath, I. T.; Kim, H. S. *Organometallics* 1984, 3, 548.

Table I. Crystallographic Data for Diffraction Studies

	<i>cis</i> -1	2	3	4
empirical formula	Os ₃ SO ₁₀ C ₂₅ H ₁₄	Os ₃ SO ₁₀ C ₂₅ H ₁₄	Os ₃ SO ₇ C ₂₂ H ₁₄	Os ₃ SO ₁₁ C ₂₆ H ₁₄ ·0.5CH ₂ Cl ₂
MW	1077.04	1077.04	802.81	1105.04
cryst syst	monoclinic	monoclinic	monoclinic	triclinic
lattice parameters				
<i>a</i> , Å	8.674 (2)	13.845 (2)	8.337 (1)	14.319 (2)
<i>b</i> , Å	35.09 (1)	14.545 (4)	17.311 (4)	17.794 (5)
<i>c</i> , Å	9.449 (2)	28.907 (6)	16.409 (3)	12.257 (4)
α, deg				106.69 (2)
β, deg	106.41 (1)	98.88 (1)	100.82 (1)	90.74 (2)
γ, deg				82.56 (2)
<i>V</i> , Å ³	2759 (1)	5751 (2)	2326.1 (8)	1784 (1)
space group	<i>P</i> ₂ ₁ / <i>c</i> (No. 14)	<i>C</i> ₂ / <i>c</i> (No. 15)	<i>P</i> ₂ ₁ / <i>c</i> (No. 14)	<i>P</i> ₁ (No. 2)
<i>Z</i>	4	8	4	4
<i>D</i> _{calc} , g/cm ³	2.59	2.49	2.29	2.58
<i>F</i> (000)	1952	3904	1480	2101
μ(Mo Kα), cm ⁻¹	139.2	133.6	110.5	130.5
temp, °C	20	20	20	20
2θ _{max} , deg	42.0	43.0	43.0	40.0
no. observns (<i>I</i> > 3σ(<i>I</i>))	2053	2519	2299	4020
no. variables	302	352	289	627
residuals: <i>R</i> , <i>R</i> _w	0.033, 0.032	0.027, 0.028	0.036, 0.040	0.041, 0.043
goodness of fit indicator	1.24	1.35	2.32	1.77
max shift in final cycle	0.05	0.04	0.00	0.01
largest peak in final diff map, e ⁻ /Å ³	1.27	0.53	1.32	1.07
abs corr	empirical	empirical	empirical	analytical

(25 mg, 0.03 mmol) in 1 mL of CDCl₃ was placed in a 5-mm NMR tube. One equivalent of *trans*-2,4-DPT (6.7 mg, 0.029 mmol) was dissolved in 0.5 mL of CDCl₃ and the resultant mixture added to the solution. The tube was shaken to mix the reactants and quickly placed in the NMR probe. The initial spectrum of the reaction mixture (taken approximately 5 min after starting) displayed resonances for unreacted *trans*-2,4-DPT ligand, *cis*- and *trans*-1 (1/1 ratio), and Os₃(CO)₁₁[SC(H)PhCH₂C(H)Ph] (7). The latter formed due to the presence of a small amount of Os₃(CO)₁₁(NCMe) impurity in the starting material (see below). After 1 h, the resonances for unreacted *trans*-2,4-DPT ligand were no longer present and the *cis*- to *trans*-1 ratio was 1.7/1. In subsequent spectra, the relative amount of *cis*- to *trans*-1 slowly increased. All of the *trans*-1 had isomerized to *cis*-1 after 72 h. At no time during the course of the reaction were the resonances of the free molecule *cis*-2,4-DPT observed.

Reaction of Os₃(CO)₁₁(NCMe) with *trans*-2,4-DPT. A solution of Os₃(CO)₁₁(NCMe) (10 mg, 0.011 mmol) in 0.5 mL of CD₂Cl₂ was placed in a 5-mm NMR tube. *trans*-2,4-DPT (2.4 mg, 0.011 mmol) dissolved in 0.5 mL of CD₂Cl₂ was added to the solution at 25 °C. The reaction was monitored by ¹H NMR. After 2.5 h, the solvent was removed in vacuo and the residue was chromatographed by TLC (4/1 hexane/CH₂Cl₂) to yield yellow Os₃(CO)₁₁[*trans*-2,4-SC(H)PhCH₂C(H)Ph] (7) (2.6 mg, 22%). IR, ν(CO) (cm⁻¹) in hexane for *trans*-7: 2109 (w), 2077 (w), 2057 (m), 2036 (m), 2021 (vs), 2002 (w), 1995 (m), 1983 (w), 1966 (w), 1955 (w). ¹H NMR (δ in CDCl₃) for *trans*-7: 7.56–7.36 (m, 10 H), 4.91 (dd, 2 H, ³J_{H-H} = 8.4, 10.9 Hz), 3.37–3.29 (complex multiplet, 2 H). In solution, compound 7 slowly decomposes over a period of hours at 25 °C. The principal decomposition products are Os₃(CO)₁₂ and free *trans*-2,4-DPT. Anal. Calcd for 7: C, 28.26; H, 1.28. Found: C, 28.82; H, 1.36.

Kinetics Experiments. One equivalent (12.0 mg, 0.053 mmol) of *trans*-2,4-DPT dissolved in 5 mL of CH₂Cl₂ was added dropwise to a solution of Os₃(CO)₁₀(NCMe)₂ (50 mg, 0.053 mmol) in 20 mL of CH₂Cl₂ at 25 °C. After the mixture was stirred for 1 h, the solvent was removed in vacuo. Compound 1 as a mixture of isomers was isolated by TLC, eluting with a 3/1 hexane/CH₂Cl₂ solvent mixture. The entire sample dissolved in 1 mL of CDCl₃ (approximately 0.03 M) was placed in a 5-mm NMR tube and kept at 25 °C in a constant-temperature bath. ¹H NMR spectra of the mixture were taken every 2 h over a 12-h period and then several times more over the next 12 h. The *cis* to *trans* ratio was determined by integration of the resonances at 4.03 and 5.04 ppm for the *cis*- and *trans*-1 isomers, respectively. The experiment was duplicated with similar results. The isomerization rate constant, *k* = 8.22 (2) × 10⁻⁶ s⁻¹, is an average of the rate constants determined from the data of the two independent runs.

Crystallographic Analyses. Dark red crystals of *cis*-1 were grown by slow evaporation of solvent from a concentrated hexane/CH₂Cl₂ (9/1) solution at -3 °C. Yellow crystals of 2 were grown by slow evaporation of solvent from a hexane solution at -14 °C. Yellow crystals of 3 and orange crystals of 4 were grown by slow evaporation of solvent from hexane solutions at 25 °C. The data crystals were mounted in thin-walled glass capillaries. Diffraction measurements were made on a Rigaku AFC6S fully automated four-circle diffractometer using graphite-monochromatized Mo Kα radiation. Unit cells were determined and refined from 15 randomly selected reflections obtained by using the AFC6 automatic search, center, index, and least-squares routines. Crystal data, data collection parameters, and results of the analyses are listed in Table I. All data processing was performed on a Digital Equipment Corp. VAXstation 3520 computer by using the TEXSAN structure solving program library obtained from the Molecular Structure Corp., The Woodlands, TX. Neutral atom scattering factors were calculated by the standard procedures.^{13a} Anomalous dispersion corrections were applied to all non-hydrogen atoms.^{13b} Lorentz-polarization (*Lp*) and absorption corrections were applied in each analysis. Full-matrix least-squares refinements minimized the function $\sum_{hkl} w(|F_o| - |F_c|)^2$, where $w = 1/\sigma(F)^2$, $\sigma(F) = \sigma(F_o^2)/2F_o$, and $\sigma(F_o^2) = [\sigma(I_{\text{raw}})^2 + (0.02I_{\text{net}}^2)^2]^{1/2}Lp$.

Compound *cis*-1 crystallized in the monoclinic crystal system. The space group *P*₂₁/*c* was identified uniquely based on the systematic absences observed during the collection of data. The structure was solved by a combination of direct methods (MITHRIL) and difference Fourier syntheses. All non-hydrogen atoms except the carbonyl carbons were refined with anisotropic thermal parameters. All hydrogen atom positions were calculated by assuming idealized geometries and the C-H distances equal to 0.95 Å. Their contributions were added to the structure factor calculations, but their positions were not refined.

Compound 2 crystallized in the monoclinic crystal system. The systematic absences were consistent with either of the space groups *C*₂/*c* or *Cc*. The centrosymmetric space group *C*₂/*c* was assumed and confirmed by the successful solution and refinement of the structure. The coordinates of the heavy atoms were obtained by direct methods (MITHRIL). All remaining non-hydrogen atoms were subsequently obtained from difference Fourier syntheses. All non-hydrogen atoms were refined with anisotropic thermal parameters. The hydride ligand was located crystallographically but could not be refined. The positions of all other hydrogen

(13) (a) *International Tables for X-ray Crystallography*; Kynoch Press: Birmingham, England, 1975; Vol. IV, Table 2.2B, pp 99–101. (b) *Ibid.* Table 2.3.1, pp 149–150.

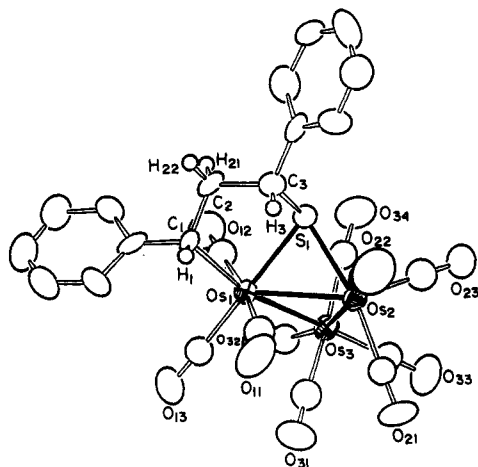


Figure 1. ORTEP diagram of $\text{Os}_3(\text{CO})_{10}[\mu\text{-SC(H)PhCH}_2\text{C(H)Ph}]$ (*cis*-1) showing 50% probability thermal ellipsoids.

atoms were calculated by assuming idealized geometries. Their contributions were added to the structure factor calculations, but their positions were not refined.

Compound 3 crystallized in the monoclinic crystal system. The space group $P2_1/c$ was identified uniquely based on the systematic absences observed during the collection of data. The structure was solved by a combination of direct methods (MITHRIL) and difference Fourier syntheses. All non-hydrogen atoms were refined with anisotropic thermal parameters. All hydrogen atom positions were calculated by assuming idealized geometries. Their contributions were added to the structure factor calculations, but their positions were not refined.

Compound 4 crystallized in the triclinic crystal system with 2 independent molecules in the asymmetric crystal unit. The centrosymmetric space group $P\bar{1}$ was assumed and confirmed as correct by the successful solution and refinement of the structure. The coordinates of the heavy atoms were obtained by direct methods (MITHRIL). All remaining non-hydrogen atoms were subsequently obtained from difference Fourier syntheses. All non-hydrogen atoms, except the carbon atoms of the phenyl rings, were refined with anisotropic thermal parameters. In the final stages of refinement, 0.5 equiv of CH_2Cl_2 of crystallization was located in the lattice and was disordered between two sites about a center of symmetry. The carbon atom and one independent chlorine atom of this molecule were satisfactorily refined. All hydrogen atom positions were calculated by assuming idealized geometries. Their contributions were added to the structure factor calculations, but their positions were not refined.

Results

The reaction of $\text{Os}_3(\text{CO})_{10}(\text{NCMe})_2$ with *trans*-2,4-DPT over a period of 1 h yielded $\text{Os}_3(\text{CO})_{10}[\mu\text{-SC(H)PhCH}_2\text{C(H)Ph}]$ (1) (76%). A ^1H NMR analysis of the product showed that it was a mixture of two isomers identified as *cis* and *trans* forms in a ratio of 1.7/1.0; see below. The formation of small amounts of $\text{Os}_3(\text{CO})_{11}[\text{trans-2,4-SC(H)PhCH}_2\text{C(H)Ph}]$ (7) is believed to be due to the presence of $\text{Os}_3(\text{CO})_{11}\text{NCMe}$ impurity in the $\text{Os}_3(\text{CO})_{10}(\text{NCMe})_2$. Compound 7 was made independently in 22% yield by the reaction of *trans*-2,4-DPT with $\text{Os}_3(\text{CO})_{11}\text{NCMe}$. The IR spectrum of 7 is virtually identical to that of $\text{Os}_3(\text{CO})_{11}[\text{S}(\text{CH}_2)_3]$ (8), which we have synthesized and structurally characterized previously.⁴ Thus, we feel that 7 and 8 are structurally similar, with the thietane ligand occupying an equatorial coordination site in the triosmium cluster.

Due to the continuous isomerization of *trans*-1 to *cis*-1, we were unable to isolate *trans*-1 in a pure form. On the other hand, *cis*-1 was isolated in a pure form and was characterized by IR, ^1H NMR, and single-crystal X-ray diffraction analyses. An ORTEP drawing of the molecular

Table II. Positional Parameters and $B(\text{eq})$ Values (\AA^2) for *cis*-1

atom	x	y	z	B(eq)
Os(1)	0.85862 (08)	0.36028 (02)	0.24532 (08)	2.54 (3)
Os(2)	0.69507 (08)	0.33337 (02)	-0.04143 (08)	2.76 (3)
Os(3)	0.57666 (08)	0.31296 (02)	0.19663 (08)	2.79 (3)
S(1)	0.6930 (05)	0.39741 (13)	0.0484 (05)	2.6 (2)
O(11)	1.0947 (16)	0.3232 (05)	0.1010 (18)	6.8 (9)
O(12)	0.6941 (16)	0.4047 (04)	0.4478 (15)	5.7 (8)
O(13)	1.0574 (16)	0.3135 (05)	0.5071 (15)	6.3 (8)
O(21)	0.7484 (18)	0.2493 (04)	-0.0983 (16)	5.8 (8)
O(22)	0.865 (02)	0.3544 (05)	-0.2708 (16)	8 (1)
O(23)	0.3582 (16)	0.3308 (04)	-0.2394 (16)	5.9 (7)
O(31)	0.8381 (17)	0.2516 (05)	0.2525 (16)	6.0 (8)
O(32)	0.5471 (17)	0.3114 (05)	0.5113 (16)	6.9 (9)
O(33)	0.3159 (16)	0.2545 (05)	0.0693 (16)	6.1 (8)
O(34)	0.3492 (15)	0.3815 (05)	0.1064 (18)	6.1 (8)
C(1)	1.0281 (19)	0.4092 (05)	0.2638 (18)	2.7 (8)
C(2)	0.944 (02)	0.4427 (05)	0.1722 (19)	3.1 (8)
C(3)	0.846 (02)	0.4291 (05)	0.0158 (02)	3.5 (9)
C(11)	0.990 (02)	0.3353 (06)	0.139 (02)	4.3 (4)
C(12)	0.753 (02)	0.3872 (06)	0.374 (02)	4.0 (4)
C(13)	0.979 (02)	0.3305 (06)	0.408 (02)	3.6 (4)
C(21)	0.727 (02)	0.2803 (06)	-0.076 (02)	3.5 (4)
C(22)	0.799 (02)	0.3488 (06)	-0.182 (02)	4.6 (5)
C(23)	0.487 (02)	0.3321 (06)	-0.166 (02)	4.4 (5)
C(31)	0.743 (02)	0.2748 (07)	0.234 (02)	4.4 (5)
C(32)	0.553 (02)	0.3102 (06)	0.394 (02)	4.0 (4)
C(33)	0.415 (02)	0.2768 (06)	0.115 (02)	3.6 (4)
C(34)	0.437 (02)	0.3567 (06)	0.143 (02)	3.8 (4)

Table III. Intramolecular Distances for *cis*-1^a

Os(1)-Os(2)	2.842 (1)	Os(3)-C(31)	1.92 (2)
Os(1)-Os(3)	2.884 (1)	Os(3)-C(32)	1.93 (2)
Os(1)-S(1)	2.390 (4)	Os(3)-C(33)	1.89 (2)
Os(1)-C(1)	2.23 (2)	Os(3)-C(34)	1.93 (2)
Os(1)-C(11)	1.93 (2)	S(1)-C(3)	1.82 (2)
Os(1)-C(12)	1.95 (2)	O-C(av)	1.14 (2)
Os(1)-C(13)	1.91 (2)	C(1)-C(2)	1.52 (2)
Os(2)-Os(3)	2.817 (1)	C(1)-C(101)	1.48 (2)
Os(2)-S(1)	2.404 (5)	C(2)-C(3)	1.56 (2)
Os(2)-C(21)	1.92 (2)	C(3)-C(301)	1.52 (2)
Os(2)-C(22)	1.88 (2)	C(Ph)-C(av)	1.38 (3)
Os(2)-C(23)	1.86 (2)		

^a Distances are in angstroms. Estimated standard deviations in the least significant figure are given in parentheses.

structure of *cis*-1 is shown in Figure 1. Final atomic positional parameters are listed in Table II. Selected interatomic distances and angles are listed in Tables III and IV. The molecule consists of a triangular cluster of three osmium atoms with ten carbonyl ligands. One carbonyl C(11)-O(11) is a weak semibridge: Os(1)-C(11)-O(11) = 165 (2)°, Os(2)···C(11) = 2.65 (2) Å. The others are terminal ligands. The most interesting ligand is the SC(H)PhCH₂C(H)Ph group, which forms a thiametalladi-phenylcyclopentane ring by including the metal atom Os(1). The sulfur atom is a bridge across Os(1)-Os(2), while the carbon C(1) is coordinated solely to Os(1); Os(1)-C(1) = 2.23 (2) Å. The longest metal-metal bond is the one that lies approximately *trans* to carbon atom C(1), Os(1)-Os(3) = 2.884 (1) Å, but this length is not significantly longer than that observed in $\text{Os}_3(\text{CO})_{12}$, 2.878 (3) Å.¹⁴ The metal-sulfur distances, 2.390 (4) and 2.404 (5) Å, are similar to the metal-sulfur distances, 2.40–2.46 Å, typically found for bridging thiolato ligands in triosmium cluster complexes.¹⁵ It is important to note the relative *cis* stereochemistry of the hydrogen atoms H(1) and H(3)

(14) Churchill, M. R.; DeBoer, B. G. *Inorg. Chem.* 1977, 16, 878.

(15) (a) Adams, R. D.; Babin, J. E.; Kim, H. S. *J. Am. Chem. Soc.* 1987, 109, 1414. (b) Allen, V. F.; Mason, R.; Hitchcock, P. B. *J. Organomet. Chem.* 1977, 140, 297. (c) Adams, R. D.; Dawoodi, Z.; Segmüller, B. E. *Organometallics* 1983, 2, 315.

Table IV. Intramolecular Bond Angles for *cis*-1^a

Os(2)–Os(1)–Os(3)	58.93 (3)	Os(3)–Os(2)–C(23)	89.4 (6)
Os(2)–Os(1)–S(1)	53.9 (1)	S(1)–Os(2)–C(21)	168.5 (6)
Os(2)–Os(1)–C(1)	118.0 (4)	S(1)–Os(2)–C(22)	91.8 (7)
Os(2)–Os(1)–C(11)	64.1 (6)	S(1)–Os(2)–C(23)	98.2 (7)
Os(2)–Os(1)–C(12)	123.9 (5)	Os(1)–Os(3)–Os(2)	59.79 (3)
Os(2)–Os(1)–C(13)	126.8 (6)	Os(1)–Os(3)–C(31)	79.3 (6)
Os(3)–Os(1)–S(1)	83.9 (1)	Os(1)–Os(3)–C(32)	100.9 (6)
Os(3)–Os(1)–C(1)	164.7 (4)	Os(1)–Os(3)–C(33)	162.3 (6)
Os(3)–Os(1)–C(11)	104.8 (6)	Os(1)–Os(3)–C(34)	91.4 (6)
Os(3)–Os(1)–C(12)	81.6 (6)	Os(2)–Os(3)–C(31)	84.3 (6)
Os(3)–Os(1)–C(13)	93.3 (6)	Os(2)–Os(3)–C(32)	160.7 (6)
S(1)–Os(1)–C(1)	83.1 (4)	Os(2)–Os(3)–C(33)	104.1 (6)
S(1)–Os(1)–C(11)	99.0 (6)	Os(2)–Os(3)–C(34)	86.1 (6)
S(1)–Os(1)–C(12)	86.4 (6)	Os(1)–S(1)–Os(2)	72.7 (1)
S(1)–Os(1)–C(13)	176.0 (5)	Os(1)–S(1)–C(3)	99.1 (6)
C(1)–Os(1)–C(11)	85.2 (7)	Os(2)–S(1)–C(3)	115.6 (6)
C(1)–Os(1)–C(12)	89.6 (7)	Os(1)–C(1)–C(2)	111 (1)
C(1)–Os(1)–C(13)	99.3 (7)	Os(1)–C(1)–C(101)	114 (1)
Os(1)–Os(2)–Os(3)	61.27 (3)	C(2)–C(1)–C(101)	113 (1)
Os(1)–Os(2)–S(1)	53.4 (1)	C(1)–C(2)–C(3)	111 (1)
Os(1)–Os(2)–C(21)	115.1 (5)	S(1)–C(3)–C(2)	105 (1)
Os(1)–Os(2)–C(22)	111.5 (6)	S(1)–C(3)–C(301)	111 (1)
Os(1)–Os(2)–C(23)	138.2 (6)	C(2)–C(3)–C(301)	114 (2)
Os(3)–Os(2)–S(1)	85.1 (1)	Os(1)–C–O(av)	172 (3)
Os(3)–Os(2)–C(21)	89.4 (5)	Os(2)–C–O(av)	176 (3)
Os(3)–Os(2)–C(22)	172.6 (6)	Os(3)–C–O(av)	177 (3)

^a Angles are in degrees. Estimated standard deviations in the least significant figure are given in parentheses.

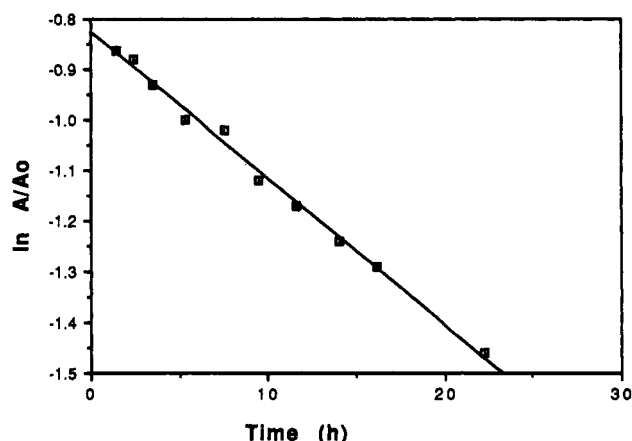


Figure 2. Log plot of the isomerization of *trans*-1 to *cis*-1 as a function of time.

and the phenyl groups on the carbon atoms C(1) and C(3), which contrasts with the *trans* stereochemistry in the thietane reagent.

The evidence for the existence of *trans*-1 was obtained by following the reaction by ¹H NMR spectroscopy. After a reaction period of only 5 min, the spectrum showed the presence of two species in approximately a 1/1 ratio, which can be attributed to a mixture of *cis*-1 and *trans*-1. It is noteworthy that there was no evidence for the formation of the free molecule *cis*-2,4-DPT during the course of this reaction. The stereochemical assignment for *trans*-1 is based primarily on the observed couplings between the hydrogen atoms on the chain of three carbon atoms in the thiametallacyclopentane ring [δ 5.04 (dd, 1 H, SCH, ³J_{H-H} = 4.6 Hz, ³J_{H-H} = 6.7 Hz), 3.68 (dd, 1 H, OsCH, ³J_{H-H} = 4.6 Hz, ³J_{H-H} = 9.9 Hz), 3.58 (dt, 1 H, CHH, ³J_{H-H} = 4.7 Hz, ³J_{H-H} = 4.7 Hz, ²J_{H-H} = 14.6 Hz), 2.75 (ddd, 1 H, CHH, ³J_{H-H} = 6.7 Hz, ³J_{H-H} = 9.7 Hz, ²J_{H-H} = 14.6 Hz] and by the fact that it slowly isomerizes to *cis*-1. This isomerization was quantitative and was thus subjected to a kinetic analysis by following the transformation of mixtures of 1 that were separated shortly after the mixing of the reagents. It was found that the isomerization was first order

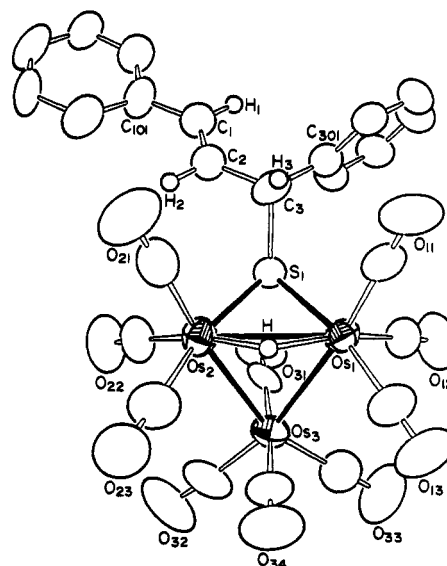


Figure 3. ORTEP diagram of Os₃(CO)₁₀[μ-SC(H)PhC(H)=C(H)Ph](μ-H) (2) showing 50% probability thermal ellipsoids.

Table V. Positional Parameters for 2

atom	x	y	z
Os(1)	0.35549 (04)	0.04699 (03)	0.663275 (18)
Os(2)	0.27698 (04)	0.21441 (03)	0.692956 (18)
Os(3)	0.15521 (04)	0.05671 (04)	0.675536 (18)
S(1)	0.3041 (02)	0.17726 (19)	0.61491 (10)
O(11)	0.5745 (08)	0.0615 (08)	0.6592 (05)
O(12)	0.3041 (08)	-0.0916 (07)	0.5850 (04)
O(13)	0.3901 (08)	-0.1044 (07)	0.7366 (04)
O(21)	0.4272 (09)	0.3671 (07)	0.7110 (04)
O(22)	0.0999 (08)	0.3337 (07)	0.6585 (04)
O(23)	0.2457 (09)	0.2205 (08)	0.7943 (04)
O(31)	0.0857 (07)	0.1223 (07)	0.5742 (03)
O(32)	-0.0372 (09)	0.1267 (10)	0.6995 (04)
O(33)	0.1079 (08)	-0.1425 (07)	0.6487 (05)
O(34)	0.2300 (08)	0.0075 (08)	0.7786 (04)
C(1)	0.3865 (09)	0.3916 (09)	0.5561 (04)
C(2)	0.3829 (09)	0.3388 (08)	0.5918 (04)
C(3)	0.4092 (09)	0.2388 (08)	0.5970 (04)
C(11)	0.4913 (11)	0.0562 (09)	0.6604 (05)
C(12)	0.3253 (10)	-0.0383 (09)	0.6141 (05)
C(13)	0.3773 (10)	-0.0467 (09)	0.7085 (06)
C(21)	0.3719 (11)	0.3100 (10)	0.7034 (05)
C(22)	0.1678 (11)	0.2922 (10)	0.6717 (05)
C(23)	0.2558 (11)	0.2164 (11)	0.7551 (06)
C(31)	0.1141 (08)	0.0989 (09)	0.6113 (05)
C(32)	0.0343 (12)	0.0969 (12)	0.6905 (05)
C(33)	0.1238 (10)	-0.0673 (11)	0.6583 (06)
C(34)	0.2007 (10)	0.0276 (09)	0.7403 (05)

in the concentration of *trans*-1 with a rate constant of $8.22 \times 10^{-6} \text{ s}^{-1}$ at 25 °C. The half-life for this transformation is thus 23.4 h. A log plot of the isomerization of *trans*-1 to *cis*-1 is shown in Figure 2.

When a solution of 1 was heated to 97 °C under an atmosphere of carbon monoxide for 1 h, five compounds were formed, which include three new complexes, Os₃(CO)₁₀[μ-SC(H)PhC(H)=C(H)Ph](μ-H) (2) (22%), Os₂(CO)₇[μ-SC(H)(C₆H₄)CH₂CH₂Ph] (3) (11%), and Os₃(CO)₁₁[μ-SC(H)PhC(H)C(H)Ph] (4) (39%), and two known compounds, the red isomer of H₂Os₆(CO)₁₇(μ₃-S)(μ₄-S) (5)¹¹ (only a trace amount) and Os₃(CO)₁₂. Compounds 3 and 5 appear to be derived from compound 2 and were obtained in better yields with the additional formation of the known compound Os₃(CO)₉(μ₃-CO)(μ₃-S) (6)¹² by heating 2 to 125 °C in octane solvent. Compound 4 is a CO adduct of 1 and an isomer of 7. Compounds 2–4 were characterized by IR, ¹H NMR, and single-crystal X-ray diffraction analyses.

Table VI. Intramolecular Distances for 2^a

Os(1)–Os(2)	2.8522 (9)	O–C(av)	1.15 (2)
Os(1)–Os(3)	2.8526 (8)	C(1)–C(2)	1.29 (2)
Os(1)–S(1)	2.397 (3)	C(1)–C(101)	1.46 (2)
Os(1)–C(11)	1.90 (2)	C(2)–C(3)	1.50 (2)
Os(1)–C(12)	1.88 (1)	C(3)–C(301)	1.51 (2)
Os(1)–C(13)	1.88 (2)	C(101)–C(102)	1.36 (2)
Os(1)–H	1.73	C(101)–C(106)	1.40 (2)
Os(2)–Os(3)	2.8451 (9)	C(102)–C(103)	1.36 (2)
Os(2)–S(1)	2.405 (3)	C(103)–C(104)	1.35 (2)
Os(2)–C(21)	1.90 (2)	C(104)–C(105)	1.38 (2)
Os(2)–C(22)	1.91 (2)	C(105)–C(106)	1.39 (2)
Os(2)–C(23)	1.86 (2)	C(301)–C(302)	1.37 (2)
Os(2)–H	1.62	C(301)–C(306)	1.38 (2)
Os(3)–C(31)	1.95 (1)	C(302)–C(303)	1.38 (2)
Os(3)–C(32)	1.89 (2)	C(303)–C(304)	1.36 (2)
Os(3)–C(33)	1.90 (2)	C(304)–C(305)	1.34 (2)
Os(3)–C(34)	1.93 (2)	C(305)–C(306)	1.38 (2)
S(1)–C(3)	1.85 (1)		

^a Distances are in angstroms. Estimated standard deviations in the least significant figure are given in parentheses.

Table VII. Intramolecular Bond Angles for 2^a

Os(2)–Os(1)–Os(3)	59.83 (2)	S(1)–Os(2)–C(21)	96.3 (4)
Os(2)–Os(1)–S(1)	53.69 (8)	S(1)–Os(2)–C(22)	93.5 (4)
Os(2)–Os(1)–C(11)	112.2 (4)	S(1)–Os(2)–C(23)	167.9 (5)
Os(2)–Os(1)–C(12)	137.6 (4)	S(1)–Os(2)–H	82.78
Os(2)–Os(1)–C(13)	116.0 (5)	C(21)–Os(2)–H	98.39
Os(2)–Os(1)–H	30.51	C(22)–Os(2)–H	165.08
Os(3)–Os(1)–S(1)	80.01 (8)	C(23)–Os(2)–H	87.71
Os(3)–Os(1)–C(11)	171.7 (4)	Os(1)–Os(3)–Os(2)	60.08 (2)
Os(3)–Os(1)–C(12)	91.1 (4)	Os(1)–Os(3)–C(31)	92.5 (3)
Os(3)–Os(1)–C(13)	90.3 (4)	Os(1)–Os(3)–C(32)	163.4 (5)
Os(3)–Os(1)–H	73.56	Os(1)–Os(3)–C(33)	96.2 (4)
S(1)–Os(1)–C(11)	97.2 (4)	Os(1)–Os(3)–C(34)	86.1 (4)
S(1)–Os(1)–C(12)	94.0 (4)	Os(2)–Os(3)–C(31)	89.6 (4)
S(1)–Os(1)–C(13)	168.5 (5)	Os(2)–Os(3)–C(32)	103.4 (5)
S(1)–Os(1)–H	80.98	Os(2)–Os(3)–C(33)	156.3 (4)
C(11)–Os(1)–H	98.35	Os(2)–Os(3)–C(34)	84.8 (4)
C(12)–Os(1)–H	164.47	Os(1)–S(1)–Os(2)	72.88 (9)
C(13)–Os(1)–H	90.47	Os(1)–S(1)–C(3)	111.7 (4)
Os(1)–Os(2)–Os(3)	60.09 (2)	Os(2)–S(1)–C(3)	113.4 (4)
Os(1)–Os(2)–S(1)	53.43 (7)	C(2)–C(1)–C(101)	126 (1)
Os(1)–Os(2)–C(21)	112.7 (4)	C(1)–C(2)–C(3)	128 (1)
Os(1)–Os(2)–C(22)	136.7 (4)	S(1)–C(3)–C(2)	108 (1)
Os(1)–Os(2)–C(23)	115.3 (5)	S(1)–C(3)–C(301)	109.7 (8)
Os(1)–Os(2)–H	32.76	C(2)–C(3)–C(301)	116 (1)
Os(3)–Os(2)–S(1)	80.03 (7)	Os(1)–C–O(av)	178 (1)
Os(3)–Os(2)–C(21)	172.7 (4)	Os(2)–C–O(av)	177 (1)
Os(3)–Os(2)–C(22)	90.2 (4)	Os(3)–C–O(av)	177 (1)
Os(3)–Os(2)–C(23)	90.3 (5)		
Os(3)–Os(2)–H	74.99		

^a Angles are in degrees. Estimated standard deviations in the least significant figure are given in parentheses.

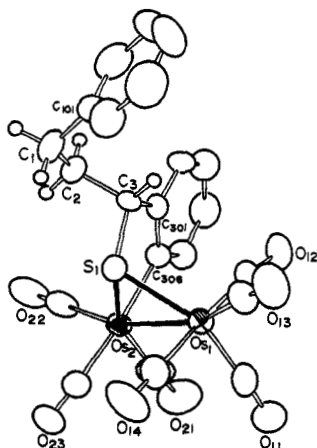


Figure 4. ORTEP diagram of $\text{Os}_2(\text{CO})_7[\mu\text{-SC(H)(C}_6\text{H}_4\text{)CH}_2\text{C(H)Ph}]$ (3) showing 50% probability thermal ellipsoids.

Table VIII. Positional Parameters and $B(\text{eq})$ Values (\AA^2) for 3

atom	x	y	z	$B(\text{eq})$
Os(1)	0.28932 (06)	0.12885 (03)	0.47341 (03)	3.23 (2)
Os(2)	0.03774 (06)	0.17848 (03)	0.34265 (04)	3.40 (3)
S(1)	0.2407 (04)	0.25891 (17)	0.4198 (02)	3.7 (2)
O(11)	0.1662 (15)	−0.0344 (07)	0.4828 (10)	9.2 (8)
O(12)	0.4951 (13)	0.0627 (06)	0.3522 (07)	5.9 (5)
O(13)	0.5986 (15)	0.1282 (07)	0.6080 (09)	7.8 (7)
O(14)	0.0881 (15)	0.1817 (08)	0.6020 (08)	8.4 (8)
O(21)	−0.1029 (15)	0.0208 (07)	0.2866 (09)	8.9 (8)
O(22)	−0.1483 (14)	0.2742 (09)	0.2044 (09)	9.4 (8)
O(23)	−0.2256 (14)	0.2050 (07)	0.4479 (08)	7.1 (7)
C(1)	0.4019 (18)	0.4249 (07)	0.3690 (10)	5.2 (7)
C(2)	0.3327 (16)	0.3631 (07)	0.3109 (10)	4.4 (6)
C(3)	0.3701 (13)	0.2802 (07)	0.3442 (09)	3.6 (6)
C(11)	0.2203 (19)	0.0285 (09)	0.4821 (11)	5.6 (8)
C(12)	0.4153 (16)	0.0920 (07)	0.3910 (09)	3.6 (6)
C(13)	0.4854 (19)	0.1315 (08)	0.5561 (10)	4.7 (7)
C(14)	0.1627 (20)	0.1623 (08)	0.5560 (10)	5.0 (7)
C(21)	−0.0562 (18)	0.0806 (10)	0.3059 (09)	5.3 (8)
C(22)	−0.0784 (16)	0.2397 (09)	0.2577 (10)	4.7 (7)
C(23)	−0.1251 (18)	0.1949 (08)	0.4129 (11)	4.6 (7)

Table IX. Intramolecular Distances for 3^a

Os(1)–Os(2)	2.8375 (9)	O–C(av)	1.13 (2)
Os(1)–S(1)	2.423 (3)	C(1)–C(2)	1.48 (2)
Os(1)–C(11)	1.84 (2)	C(1)–C(101)	1.50 (2)
Os(1)–C(12)	1.97 (1)	C(2)–C(3)	1.55 (2)
Os(1)–C(13)	1.92 (2)	C(3)–C(301)	1.51 (2)
Os(1)–C(14)	1.95 (2)	C(301)–C(302)	1.38 (2)
Os(2)–S(1)	2.367 (3)	C(301)–C(306)	1.40 (2)
Os(2)–C(21)	1.92 (2)	C(302)–C(303)	1.36 (2)
Os(2)–C(22)	1.87 (2)	C(303)–C(304)	1.37 (2)
Os(2)–C(23)	1.96 (2)	C(304)–C(305)	1.38 (2)
Os(2)–C(306)	2.17 (1)	C(305)–C(306)	1.38 (2)
S(1)–C(3)	1.83 (1)	C(Ph)–C(av)	1.35 (3)

^a Distances are in angstroms. Estimated standard deviations in the least significant figure are given in parentheses.

Table X. Intramolecular Bond Angles for 3^a

Os(2)–Os(1)–S(1)	52.76 (8)	C(23)–Os(2)–C(306)	174.1 (5)
Os(2)–Os(1)–C(11)	98.4 (5)	Os(1)–S(1)–Os(2)	72.64 (9)
Os(2)–Os(1)–C(12)	89.6 (4)	Os(1)–S(1)–C(3)	110.7 (4)
Os(2)–Os(1)–C(13)	159.7 (4)	Os(2)–S(1)–C(3)	102.0 (4)
Os(2)–Os(1)–C(14)	90.9 (4)	C(2)–C(1)–C(101)	115 (1)
S(1)–Os(1)–C(11)	150.5 (5)	C(1)–C(2)–C(3)	115 (1)
S(1)–Os(1)–C(12)	97.3 (4)	S(1)–C(3)–C(2)	108.7 (9)
S(1)–Os(1)–C(13)	107.3 (4)	S(1)–C(3)–C(301)	112.1 (8)
S(1)–Os(1)–C(14)	84.3 (4)	C(2)–C(3)–C(301)	111 (1)
Os(1)–Os(2)–S(1)	54.60 (8)	Os–C–O(av)	175 (2)
Os(1)–Os(2)–C(21)	99.8 (5)	C(3)–C(301)–C(302)	118 (1)
Os(1)–Os(2)–C(22)	160.3 (4)	C(3)–C(301)–C(306)	121 (1)
Os(1)–Os(2)–C(23)	95.4 (4)	C(302)–C(301)–C(306)	121 (1)
Os(1)–Os(2)–C(306)	88.2 (3)	C(301)–C(302)–C(303)	119 (1)
S(1)–Os(2)–C(21)	153.8 (5)	C(302)–C(303)–C(304)	122 (2)
S(1)–Os(2)–C(22)	106.5 (4)	C(303)–C(304)–C(305)	118 (1)
S(1)–Os(2)–C(23)	96.0 (4)	C(304)–C(305)–C(306)	123 (1)
S(1)–Os(2)–C(306)	82.3 (4)	Os(2)–C(306)–C(301)	118 (1)
C(21)–Os(2)–C(306)	92.5 (6)	Os(2)–C(306)–C(305)	125 (1)
C(22)–Os(2)–C(306)	83.0 (5)	C(301)–C(306)–C(305)	117 (1)

^a Angles are in degrees. Estimated standard deviations in the least significant figure are given in parentheses.

An ORTEP drawing of the molecular structure of 2 is shown in Figure 3. Final atomic positional parameters are listed in Table V. Selected interatomic distances and angles are listed in Tables VI and VII. The molecule consists of a triosmium cluster with 10 linear terminal carbonyl ligands. There is a bridging 1,3-diphenylpropenethiolato and a bridging hydride ligand across the Os(1)–Os(2) bond, Os(1)–Os(2) = 2.8522 (9) Å. The C(1)–C(2) distance in the propenyl group is short, 1.29 (2) Å, consistent with its double-bond character while the C(2)–C(3) bond is long, 1.50 (2) Å, as expected. Overall, the cluster is structurally very similar to related triosmium

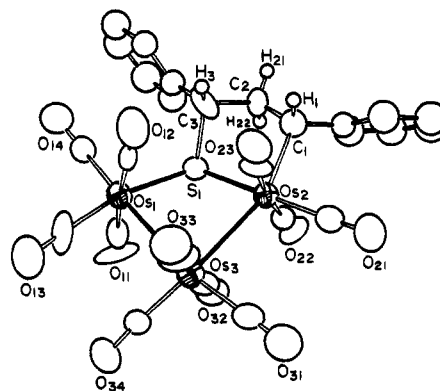
Table XI. Positional Parameters and *B*(eq) Values (Å²) for **4**

atom	<i>x</i>	<i>y</i>	<i>z</i>	<i>B</i> (eq)
Os(1A)	0.56345 (07)	0.17398 (07)	0.60265 (09)	4.25 (6)
Os(1B)	0.03628 (07)	0.19255 (07)	1.12322 (08)	3.46 (5)
Os(2A)	0.49792 (07)	0.30872 (06)	0.39736 (08)	3.18 (5)
Os(2B)	0.06597 (07)	0.31127 (06)	0.89830 (08)	3.22 (5)
Os(3A)	0.41793 (07)	0.31156 (07)	0.62149 (08)	3.65 (5)
Os(3B)	0.14456 (07)	0.32466 (06)	1.12751 (08)	3.43 (5)
S(1A)	0.6230 (04)	0.2374 (04)	0.4730 (05)	3.5 (3)
S(1B)	-0.0390 (04)	0.2448 (04)	0.9783 (05)	3.3 (3)
O(11A)	0.6577 (15)	0.2968 (14)	0.7889 (16)	7 (1)
O(11B)	-0.1042 (13)	0.3195 (13)	1.2852 (19)	7 (1)
O(12A)	0.4644 (17)	0.0626 (14)	0.4085 (20)	8 (1)
O(12B)	-0.0838 (16)	0.0593 (13)	1.0989 (16)	7 (1)
O(13A)	0.4511 (18)	0.1285 (19)	0.782 (02)	11 (2)
O(13B)	0.1435 (14)	0.1617 (13)	1.3272 (17)	7 (1)
O(14A)	0.7308 (17)	0.0433 (15)	0.5808 (20)	9 (2)
O(14B)	0.1862 (15)	0.0826 (12)	0.9537 (17)	7 (1)
O(21A)	0.3571 (12)	0.4139 (11)	0.3015 (16)	5 (1)
O(21B)	0.1816 (13)	0.4111 (12)	0.8020 (16)	6 (1)
O(22A)	0.6066 (14)	0.4514 (14)	0.4785 (17)	7 (1)
O(22B)	-0.0893 (13)	0.4547 (11)	0.9670 (15)	6 (1)
O(23A)	0.3825 (14)	0.1767 (13)	0.2791 (17)	7 (1)
O(23B)	0.2146 (14)	0.1751 (13)	0.7888 (16)	6 (1)
O(31A)	0.2720 (14)	0.4431 (13)	0.5893 (16)	6 (1)
O(31B)	0.2566 (13)	0.4514 (12)	1.0885 (16)	6 (1)
O(32A)	0.5591 (14)	0.4342 (13)	0.7094 (16)	7 (1)
O(32B)	0.3161 (12)	0.2070 (12)	1.0225 (16)	6 (1)
O(33A)	0.2824 (16)	0.1887 (14)	0.5150 (18)	8 (1)
O(33B)	-0.0290 (15)	0.4440 (13)	1.1993 (17)	7 (1)
O(34A)	0.3604 (13)	0.3153 (14)	0.8625 (18)	7 (1)
O(34B)	0.2031 (13)	0.3322 (12)	1.3734 (15)	6 (1)
C(1A)	0.5908 (16)	0.2657 (13)	0.2416 (18)	3 (1)
C(1B)	-0.0154 (15)	0.2653 (15)	0.7409 (19)	4 (1)
C(2A)	0.6857 (16)	0.2298 (16)	0.2701 (18)	4 (1)
C(2B)	-0.0969 (16)	0.2237 (14)	0.7690 (19)	4 (1)
C(3A)	0.6812 (15)	0.1690 (16)	0.3402 (18)	4 (1)
C(3B)	-0.0765 (17)	0.1733 (16)	0.8498 (18)	4 (1)
C(11A)	0.626 (02)	0.2527 (19)	0.721 (02)	6 (2)
C(11B)	-0.0535 (19)	0.2728 (18)	1.231 (02)	4 (2)
C(12A)	0.495 (02)	0.1061 (19)	0.483 (03)	6 (2)
C(12B)	-0.0437 (18)	0.1138 (16)	1.1082 (19)	4 (1)
C(13A)	0.495 (02)	0.1447 (19)	0.717 (03)	7 (2)
C(13B)	0.1055 (18)	0.1711 (16)	1.248 (02)	5 (2)
C(14A)	0.668 (02)	0.0993 (20)	0.591 (02)	6 (2)
C(14B)	0.1312 (16)	0.1262 (17)	1.019 (02)	4 (1)
C(21A)	0.4091 (18)	0.3750 (17)	0.3387 (19)	4 (1)
C(21B)	0.1386 (17)	0.3717 (16)	0.843 (02)	4 (1)
C(22A)	0.5660 (18)	0.3971 (19)	0.449 (02)	5 (2)
C(22B)	-0.0348 (17)	0.4014 (16)	0.9459 (20)	3.4 (5)
C(23A)	0.4235 (17)	0.2243 (18)	0.328 (02)	4 (2)
C(23B)	0.1606 (17)	0.2242 (18)	0.835 (02)	4 (1)
C(31A)	0.326 (02)	0.3942 (19)	0.601 (02)	5 (2)
C(31B)	0.2125 (19)	0.4040 (18)	1.100 (02)	5 (2)
C(32A)	0.5105 (18)	0.3853 (17)	0.674 (02)	4 (1)
C(32B)	0.2491 (18)	0.2492 (16)	1.062 (02)	4 (1)
C(33A)	0.3305 (18)	0.2336 (17)	0.5541 (20)	4 (1)
C(33B)	0.0340 (17)	0.3957 (19)	1.172 (02)	5 (2)
C(34A)	0.3838 (17)	0.3111 (18)	0.769 (03)	5 (2)
C(34B)	0.1825 (16)	0.3322 (15)	1.281 (02)	4 (1)

cluster complexes that contain bridging thiolato ligands.¹⁵

An ORTEP drawing of the molecular structure of **3** is shown in Figure 4. Final atomic positional parameters are listed in Table VIII. Selected interatomic distances and angles are listed in Tables IX and X. Compound **3** contains only two osmium atoms. There are seven linear terminal carbonyl ligands and a 1,3-diphenylpropane-thiolato ligand that bridges the metal-metal bond via the sulfur atom and has the phenyl group in the 1-position orthometalated to Os(2), Os(2)-C(306) = 2.17 (1) Å.

An ORTEP drawing of **4** is shown in Figure 5. Final atomic positional parameters are listed in Table XI. Selected interatomic distances and angles are listed in Tables XII and XIII. The crystal contains 2 symmetry-independent molecules in its asymmetric unit, but both

**Figure 5.** ORTEP diagram of Os₃(CO)₁₁[μ-SC(H)PhCH₂C(H)Ph] (**4**) showing 50% probability thermal ellipsoids.**Table XII.** Intramolecular Distances for **4**^a

Os(1A)-Os(3A)	2.959 (2)	Os(2B)-Os(3B)	2.970 (2)
Os(1A)-Os(2A)	3.973 (2)	Os(2B)-S(1B)	2.406 (6)
Os(1A)-S(1A)	2.417 (6)	Os(2B)-C(1B)	2.24 (2)
Os(1A)-C(11A)	2.00 (4)	Os(2B)-C(21B)	1.85 (3)
Os(1A)-C(12A)	1.95 (3)	Os(2B)-C(22B)	1.97 (3)
Os(1A)-C(13A)	1.94 (4)	Os(2B)-C(23B)	1.91 (3)
Os(1A)-C(14A)	1.84 (3)	Os(3A)-C(31A)	1.91 (3)
Os(1B)-Os(3B)	2.967 (2)	Os(3A)-C(32A)	1.96 (3)
Os(1B)-Os(2B)	3.981 (2)	Os(3A)-C(33A)	1.98 (3)
Os(1B)-S(1B)	2.412 (6)	Os(3A)-C(34A)	1.88 (3)
Os(1B)-C(11B)	1.98 (3)	Os(3B)-C(31B)	1.92 (3)
Os(1B)-C(12B)	1.89 (3)	Os(3B)-C(32B)	1.89 (3)
Os(1B)-C(13B)	1.91 (3)	Os(3B)-C(33B)	1.87 (3)
Os(1B)-C(14B)	1.91 (3)	Os(3B)-C(34B)	1.92 (3)
Os(2A)-Os(3A)	2.975 (2)	C(1A)-C(2A)	1.51 (3)
Os(2A)-S(1A)	2.392 (6)	C(1B)-C(2B)	1.55 (3)
Os(2A)-C(1A)	2.23 (2)	C(2A)-C(3A)	1.57 (3)
Os(2A)-C(21A)	1.90 (3)	C(2B)-C(3B)	1.52 (3)
Os(2A)-C(22A)	1.91 (3)	C-O(av)	1.13 (3)
Os(2A)-C(23A)	1.94 (3)	C _{ring} -C(av)	1.40 (3)

^a Distances are in angstroms. Estimated standard deviations in the least significant figure are given in parentheses.

Table XIII. Intramolecular Bond Angles for **4**^a

Os(3A)-Os(1A)-S(1A)	77.2 (2)	Os(1A)-Os(3A)-Os(2A)	84.06 (5)
Os(3A)-Os(1A)-C(11A)	82.9 (7)	Os(1A)-Os(3A)-C(31A)	168.4 (9)
Os(3A)-Os(1A)-C(12A)	92 (1)	Os(1A)-Os(3A)-C(32A)	91.3 (7)
Os(3A)-Os(1A)-C(13A)	89.9 (9)	Os(1A)-Os(3A)-C(33A)	86.6 (8)
Os(3A)-Os(1A)-C(14A)	171 (1)	Os(1A)-Os(3A)-C(34A)	90.4 (8)
S(1A)-Os(1A)-C(11A)	84.3 (9)	Os(2A)-Os(3A)-C(31A)	85.4 (9)
S(1A)-Os(1A)-C(12A)	92.8 (8)	Os(2A)-Os(3A)-C(32A)	80.8 (7)
S(1A)-Os(1A)-C(13A)	166.9 (9)	Os(2A)-Os(3A)-C(33A)	94.2 (6)
S(1A)-Os(1A)-C(14A)	95.9 (8)	Os(2A)-Os(3A)-C(34A)	172.5 (7)
Os(3B)-Os(1B)-S(1B)	77.9 (1)	Os(1B)-Os(3B)-Os(2B)	84.23 (4)
Os(3B)-Os(1B)-C(11B)	86.2 (7)	Os(1B)-Os(3B)-C(31B)	169.5 (7)
Os(3B)-Os(1B)-C(12B)	172.5 (7)	Os(1B)-Os(3B)-C(32B)	88.8 (7)
Os(3B)-Os(1B)-C(13B)	91.2 (7)	Os(1B)-Os(3B)-C(33B)	89.1 (9)
Os(3B)-Os(1B)-C(14B)	86.5 (8)	Os(1B)-Os(3B)-C(34B)	91.4 (7)
S(1B)-Os(1B)-C(11B)	85.5 (7)	Os(2B)-Os(3B)-C(31B)	85.9 (7)
S(1B)-Os(1B)-C(12B)	94.7 (7)	Os(2B)-Os(3B)-C(32B)	90.5 (7)
S(1B)-Os(1B)-C(13B)	168.5 (7)	Os(2B)-Os(3B)-C(33B)	81.5 (8)
S(1B)-Os(1B)-C(14B)	92.7 (7)	Os(2B)-Os(3B)-C(34B)	174.0 (7)
Os(3A)-Os(2A)-S(1A)	77.3 (1)	Os(1A)-S(1A)-Os(2A)	111.4 (2)
Os(3A)-Os(2A)-C(1A)	157.6 (6)	Os(1A)-S(1A)-C(3A)	115.2 (9)
Os(3A)-Os(2A)-C(21A)	105.7 (7)	Os(2A)-S(1A)-C(3A)	101.3 (7)
Os(3A)-Os(2A)-C(22A)	98.0 (7)	Os(1B)-S(1B)-Os(2B)	111.5 (2)
Os(3A)-Os(2A)-C(23A)	87.5 (8)	Os(1B)-S(1B)-C(3B)	117.4 (9)
S(1A)-Os(2A)-C(1A)	82.2 (6)	Os(2B)-S(1B)-C(3B)	101.6 (8)
S(1A)-Os(2A)-C(21A)	172.8 (7)	Os(2A)-C(1A)-C(2A)	110 (1)
S(1A)-Os(2A)-C(22A)	85.8 (8)	Os(2B)-C(1B)-C(2B)	110 (1)
S(1A)-Os(2A)-C(23A)	100.4 (8)	C(1A)-C(2A)-C(3A)	114 (2)
Os(3B)-Os(2B)-S(1B)	78.0 (1)	C(1B)-C(2B)-C(3B)	117 (2)
Os(3B)-Os(2B)-C(1B)	159.0 (6)	S(1A)-C(3A)-C(2A)	99 (2)
Os(3B)-Os(2B)-C(21B)	102.0 (7)	S(1A)-C(3A)-C(41A)	110 (2)
Os(3B)-Os(2B)-C(22B)	96.9 (6)	S(1B)-C(3B)-C(2B)	102 (2)
Os(3B)-Os(2B)-C(23B)	89.4 (7)		
S(1B)-Os(2B)-C(1B)	82.4 (6)		
S(1B)-Os(2B)-C(21B)	174.2 (8)		
S(1B)-Os(2B)-C(22B)	83.6 (7)		
S(1B)-Os(2B)-C(23B)	99.1 (8)		

^a Angles are in degrees. Estimated standard deviations in the least significant figure are given in parentheses.

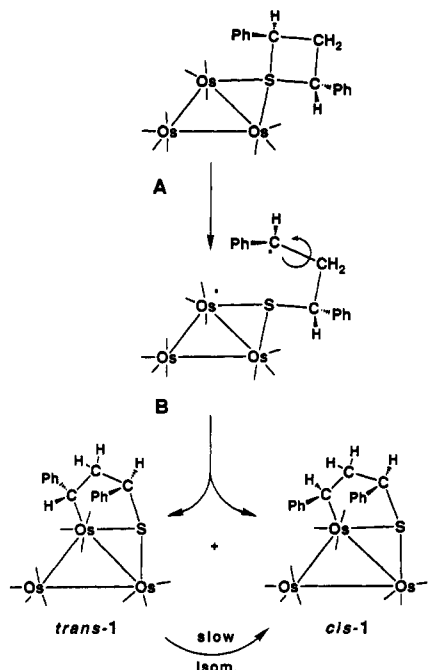


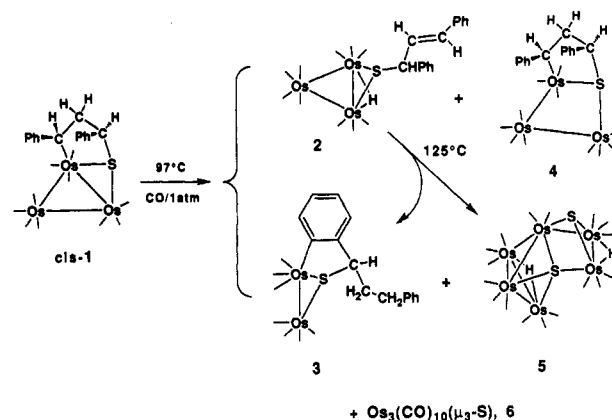
Figure 6. Possible mechanism for the ring opening of *trans*-2,4-diphenylthietane by $\text{Os}_3(\text{CO})_{10}(\text{NCMe})_2$.

molecules are essentially the same structurally. The molecule contains an open cluster of three osmium atoms with 11 linear terminal carbonyl ligands. It is simply a CO adduct of 1, but the addition of CO produces a cleavage of the sulfur-bridged metal-metal bond, $\text{Os}(1)\cdots\text{Os}(2) = 3.973(2) [3.981(2)] \text{ \AA}$. Both metal-metal bonds are of similar lengths, $2.959(2) - 2.975(2) \text{ \AA}$, and are slightly longer than those in $\text{Os}_3(\text{CO})_{12}$,¹⁴ but are very similar to the Os-Os bond lengths in $\text{Os}_3(\text{CO})_{10}(\text{PMe}_2\text{Ph})[\mu\text{-S}(\text{CH}_2)_3]$ (9), $2.9504(7)$ and $2.9559(7) \text{ \AA}$, which also contains a thiametallacyclopentane ring system in an open triosmium cluster.⁴ The thiametalladiphenylcyclopentane ring was not significantly affected by the opening of the cluster, $\text{Os}(2)-\text{C}(1) = 2.23(2) [2.24(2)] \text{ \AA}$. The coordination of the carbon and sulfur atoms is similar to that observed in 1 and the complexes 9 and $[\text{NEt}_4]^+[\text{Os}_3(\text{CO})_{10}(\mu\text{-SCH}_2\text{CMe}_2\text{CH}_2)(\mu\text{-Cl})]^-$ (10).^{4,7} As in *cis*-1 the phenyl groups in 4 also have the *cis* geometry.

Discussion

The acetonitrile ligands in $\text{Os}_3(\text{CO})_{10}(\text{NCMe})_2$ and $\text{Os}_3(\text{CO})_{11}(\text{NCMe})$ are readily displaced by *trans*-2,4-DPT to yield the new complexes 1 and 7.⁴ Compound 7 is analogous to 8 and contains simply an S-coordinated 2,4-DPT ligand. Compound 1 is formed as a mixture of two isomers, *cis* and *trans*, that differ in their relative orientation of the phenyl substituents. It was observed that *trans*-1 does isomerize to *cis*-1, but the rate of isomerization is far too slow to account for the formation of the large amounts of *cis*-1 that are formed in the first few minutes of the reaction of $\text{Os}_3(\text{CO})_{10}(\text{NCMe})_2$ with the *trans*-2,4-DPT. Since *trans*-2,4-DPT does not isomerize to *cis*-2,4-DPT under these conditions and since no *cis*-2,4-DPT was observed to form during the reaction, we believe that the two products are formed independently as the reaction proceeds. The formation of 1 is formally an oxidative-addition reaction¹⁶ that involves the cleavage of one of the carbon-sulfur bonds of the 2,4-DPT molecule. Carbon-

Scheme I



sulfur bond cleavage reactions by oxidative addition have been observed in the reactions of thiophenes¹⁷ and diaryl sulfides¹⁸ with metal complexes.

It is proposed that the reaction of $\text{Os}_3(\text{CO})_{10}(\text{NCMe})_2$ with *trans*-2,4-DPT proceeds initially by a simple displacement of the NCMe ligands with the *trans*-2,4-DPT. An intermediate A containing an S-coordinated bridging *trans*-2,4-DPT might be traversed but was not observed; see Figure 6. In the reaction of $\text{Os}_3(\text{CO})_{10}(\text{NCMe})_2$ with 3,3-dimethylthietane the complex $\text{Os}_3(\text{CO})_{10}(\mu\text{-SCH}_2\text{CMe}_2\text{CH}_2)$, which has precisely the structure depicted by A, was isolated and characterized.⁶ The presence of two phenyl substituents proximate to the cluster in A could destabilize this complex. The two most plausible mechanisms for the cleavage of a carbon-sulfur bond are (1) a concerted process that would be expected to proceed with a retention of stereochemistry at the carbon atom and (2) a stepwise process such as a homolysis, possibly via a diradical intermediate, such as B, that should result in a loss of stereochemistry at the carbon atom.¹⁹ Since the reaction yields essentially equimolar amounts of *cis*-1 and *trans*-1 as the initially formed products, we feel that a process of the latter type is strongly indicated. The loss in stereochemistry that was observed in the opening of the *trans*-2,4-DPT ring contrasts with the metal-induced opening of the three-membered phosphirane ring in the complexes (*Z*)- and (*E*)- $\text{W}(\text{CO})_5[\text{PPhC}(\text{H})\text{PhC}(\text{H})\text{Ph}]$ where a retention of stereochemistry was observed.²⁰

We have shown previously that in some cases the opening of thietane rings is promoted by UV-vis radiation.^{4,7} We tested for that possibility by performing the reaction in complete darkness and found that it proceeded at a similar rate. Thus, light promotion is considered to be unimportant in this case. It was found that the product *trans*-1 isomerizes slowly to *cis*-1. This probably occurs by an inversion of configuration at the metal-bonded carbon atom and could take place by returning to the intermediate from which the two products were initially formed.

(17) (a) Jones, W. D.; Dong, L. *J. Am. Chem. Soc.* **1991**, *113*, 559. (b) Chen, J.; Daniels, L. M.; Angelici, R. J. *J. Am. Chem. Soc.* **1990**, *112*, 199. (c) Ogilvy, A. E.; Draganjac, M.; Rauchfuss, T. B.; Wilson, S. R. *Organometallics* **1988**, *7*, 1171. (d) Manuel, T. A.; Meyer, T.; *Inorg. Chem.* **1964**, *3*, 1049. (e) Hubener, P.; Weiss, E. *J. Organomet. Chem.* **1977**, *129*, 105.

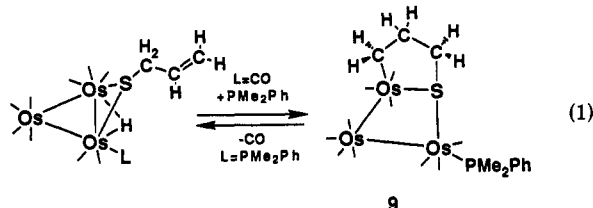
(18) Osakada, K.; Maeda, M.; Nakamura, Y.; Yamamoto, T. *J. Chem. Soc., Chem. Commun.* **1986**, 442. (g) Wenkert, E.; Shepard, M. E.; McPhail, A. T. *J. Chem. Soc., Chem. Commun.* **1986**, 1390.

(19) Efforts to detect radical-like species have been unsuccessful. Heteropolar cleavage involving zwitterionic intermediates would give an indistinguishable result.

(20) Carmichael, D.; Hitchcock, P. B.; Nixon, J. F.; Mathey, F.; Ricard, L. *J. Chem. Soc., Chem. Commun.* **1989**, 1389.

(16) Collman, J. P.; Hegedus, L. S.; Norton, J. R.; Finke, R. G. *Principles and Applications of Organotransition Metal Chemistry*; University Science Books: Mill Valley, CA, 1987; Chapter 5.

When *cis*-1 was heated to 97 °C under an atmosphere of CO, the isomer 2 and CO adduct 4 were formed. The fragmentation product 3 is also formed together with some $\text{Os}_3(\text{CO})_{12}$; see Scheme 1. The formation of 2 is formally equivalent to a " β -elimination" reaction, but it must be noted that the mechanism of the transformation has not yet been established. It has been shown that β -elimination reactions involving metallacycles in mononuclear metal complexes are energetically unfavorable.²¹ Curiously, we have also observed a facile example of the reverse of this reaction, a phosphine-promoted intramolecular insertion reaction of $\text{Os}_3(\text{CO})_{10}[\mu\text{-SCH}_2\text{C}(\text{H})=\text{CH}_2](\mu\text{-H})$ to yield 9 (eq 1).⁴ Compound 9 will also engage in a facile " β -



elimination" to yield the propenethiolato complex $\text{Os}_3(\text{CO})_9(\text{PMe}_2\text{Ph})[\mu\text{-SCH}_2\text{C}(\text{H})=\text{CH}_2](\mu\text{-H})$. Studies to try to ascertain the mechanism of these transformations are in progress.

(21) (a) Miller, T. M.; Whitesides, G. M. *Organometallics* 1986, 5, 1473. (b) McDermott, J. X.; White, J. F.; Whitesides, G. M. *J. Am. Chem. Soc.* 1976, 98, 6521.

When heated to 125 °C, compound 2 was transformed into 3, the hexanuclear compound 5, and the trinuclear compound 6. The mechanism of the fragmentation and formation of 3 is also unclear at this time, and the fate of the missing osmium carbonyl grouping was not established. Compound 5 was prepared previously by the thermal degradation of $\text{Os}_3(\text{CO})_{10}(\mu\text{-SCH}_2\text{Ph})(\mu\text{-H})$.¹¹ That reaction was shown to proceed by a homolysis of the C-S bond. A similar process is anticipated for the transformation of 2 to 5. The fate of the diphenylpropenyl grouping was not established in this reaction. Compound 6 was obtained previously by the photoinduced elimination of benzene from $\text{Os}_3(\text{CO})_{10}(\mu\text{-SPh})(\mu\text{-H})$.¹² It seems reasonable to expect that a similar thermal reaction of 2 has occurred in this case with the formation of diphenylpropene, but due to the conditions and small amounts of material involved in this reaction, the formation of diphenylpropene was not established.

Acknowledgment is made to the donors of the Petroleum Research Fund, administered by the American Chemical Society, for support of this research.

Registry No. *cis*-1, 137432-20-3; *trans*-1, 137332-96-8; 2, 137332-97-9; 3, 137332-98-0; 4, 137332-99-1; 5, 137333-00-7; 6, 88746-45-6; *trans*-2,4-DPT, 24609-88-9; $\text{Os}_3(\text{CO})_{10}(\text{NCMe})_2$, 61817-93-4.

Supplementary Material Available: Tables of phenyl ring and hydrogen atom positional parameters and anisotropic thermal parameters (22 pages); tables of observed and calculated structure factor amplitudes (76 pages). Ordering information is given on any current masthead page.

Interactions of 1,4-Diazabicyclo[2.2.2]octane with Group III Metal Trimethyls: Structures of $\text{Me}_3\text{M}\cdot\text{N}(\text{C}_2\text{H}_4)_3\text{N}\cdot\text{MMe}_3$ (M = Al, Ga)

Arleen M. Bradford, Donald C. Bradley,* Michael B. Hursthouse,* and Majid Motevalli

Department of Chemistry, Queen Mary and Westfield College, Mile End Road, London E1 4NS, United Kingdom

Received May 7, 1991

The reactions of $(\text{Me}_3\text{Al})_2$ and $\text{Me}_3\text{Ga}\cdot\text{OEt}_2$ with 1,4-diazabicyclo[2.2.2]octane (dabco) gave the Lewis acid-base complexes $\text{Me}_3\text{M}\cdot\text{N}(\text{C}_2\text{H}_4)_3\text{N}\cdot\text{MMe}_3$ (M = Al (1), Ga (2)). These complexes are discrete 2:1 adducts of the metal trialkyl to dabco. ¹H NMR spectra revealed an upfield shift of both the dabco methylene protons and the metal alkyl protons on coordination of the Lewis base. Methyl proton resonances move downfield as the metal center is varied from Al to Ga to In (comparisons being made with the previously reported complex trimethylindium 1,4-diazabicyclo[2.2.2]octane).¹ Complexes 1 and 2 were also characterized by IR spectroscopy, where it was found that the vibrational frequency for the M-C asymmetric stretching mode is lower for the adduct species than for the parent metal trimethyls. The molecular structures of 1 and 2, which are isostructural, were determined by X-ray crystallographic analysis. Crystal data for 1: trigonal, $R\bar{3}m$, $a = b = 11.223$ (2) Å, $c = 22.757$ (8) Å, $\alpha = \beta = 90^\circ$, $\gamma = 120^\circ$, $Z = 6$, $R = 0.073$. Crystal data for 2: trigonal, $R\bar{3}m$, $a = b = 11.231$ (4) Å, $c = 22.693$ (13) Å, $\alpha = \beta = 90^\circ$, $\gamma = 120^\circ$, $Z = 6$, $R = 0.043$. The molecules have 3m symmetry, and although the Al-C and Ga-C bond lengths were almost equal, the Al-N bond at 2.066 (8) Å was significantly shorter than the Ga-N bond at 2.159 (9) Å. Notable differences in volatility, solubility, and reactivity between 1 and 2 are discussed.

Introduction

The development of high-purity precursors for the preparation of III/V semiconductor materials has been of critical importance for successful device fabrication.²

Previously the realization of the full potential of techniques such as metalloorganic chemical vapor deposition (MOCVD) and organometallic vapor-phase epitaxy (OMVPE) has been delayed by the inadequacy of the source materials available. The advent of adduct pre-

(1) Bradley, D. C.; Dawes, H. M.; Frigo, D. M.; Hursthouse, M. B.; Hussain, B. *J. Organomet. Chem.* 1987, 325, 55.

(2) Cole-Hamilton, D. J. *Chem. Br.* 1990, 852.